

**Thermal poling of silica in air and under vacuum:  
the influence of charge transport on second harmonic generation**

**V. Pruneri, F. Samoggia, G. Bonfrate, P.G. Kazansky, and G.M. Yang\***

Optoelectronics Research Centre, Southampton University, Southampton, SO17 1BJ, UK

Fax: +44/1703/593149, Tel: +44/1703/593083, email: vp3@orc.soton.ac.uk

**Abstract**

A comparison between thermal poling of silica in air and in vacuum is reported. It is shown that the second-order susceptibility and thickness of the nonlinear layer as well as their time evolution are highly dependent on the surrounding poling atmosphere. In the vacuum case a charge distribution (under the anode) more complex and broader than that for the air case has also been revealed by laser induced pressure pulse measurements. A multiple charge carrier model can explain the formation and evolution of the depletion region under the anode. The findings are relevant to achieve improved nonlinearities in fibre and waveguide devices.

\*Institute for Electroacoustics, Technical University of Darmstadt, Darmstadt D-64293, Germany.

Silica is naturally an amorphous material with a macroscopic inversion symmetry that prevents second order nonlinear effects. Several poling techniques [1,2,3] have been used to break the centrosymmetry and achieve a non-zero second-order nonlinear optical susceptibility ( $\chi^{(2)}$ ). Among these, thermal poling [1] is certainly the most popular and it provides values of  $\chi^{(2)}$  ( $\sim 1$  pm/V) high enough for the realisation of important devices, such as electro-optic modulators/switches and nonlinear optical parametric converters. In addition the  $\chi^{(2)}$  region, located under the anodic surface over a thin layer ( a few  $\mu\text{m}$  up to tens of  $\mu\text{m}$ ), has shown a high degree of stability (no changes were observed after one year at room temperature), certainly higher than those obtained with other techniques, e.g. UV excited poling [4].

The mechanism behind the nonlinearity is not completely understood yet. An explanation that has been given is related to dipole alignment in the structure breaking the symmetry, but it is more common believe that  $\chi^{(2)}$  is due to the third order nonlinearity ( $\chi^{(3)}$ ) and the electrostatic field ( $E_{\text{DC}}$ ) induced by poling, i.e.  $\chi^{(2)} = 3 \chi^{(3)} E_{\text{DC}}$  . Initial studies [5] on second-harmonic-generation (SHG) from silica samples poled in air and vacuum indicated that molecular species in the atmosphere were affecting the poling process and the formation of the nonlinearity. In this paper we report systematic studies which include the measurement of  $\chi^{(2)}$  and thickness of the nonlinear layer as well as their time evolution, highlighting the influence of the surrounding atmosphere by comparing results obtained in air and in vacuum. The resulting charge distribution under the anode has also been tested by laser induced pressure pulse (LIPP) measurements and is consistent with the second-harmonic optical experiments. To explain the results we propose a model which includes the migration not only of  $\text{Na}^+$  and  $\text{H}^+$  or  $\text{H}_3\text{O}^+$  [6] but also of negative

charged carriers such as electrons [5,7] and oxygen ions [8] driven by the high electric field in the depletion region.

The experiments were carried out using ~0.1 mm thick plates of Herasil 1 supplied by Heraeus. The small sample thickness allows high resolution in the LIPP measurements and negligible beam displacement associated to angular rotation of the sample during the optical measurements. 'Pressed-contact' electrodes (silicon anode and stainless steel cathode) were used during poling. For the optical experiments we used a Q-switched and mode-locked Nd:YAG laser as fundamental source. The LIPP measurements were performed as described in references 9 and 10.

Fig. 1 shows the SH intensity as a function of poling time for silica samples thermally poled in air and vacuum ( $10^{-8}$  atm) at 290 °C and 4 kV for different times. The poling time given in this paper is the sum of the actual time at 290 °C and of the cooling time to reach temperatures of ~220 °C (the contribution to poling below this temperature can be considered not significant). The SH signals generated from samples poled in air are in general higher than those from samples poled in vacuum. This and the clear differences in the time evolution of SH signals make already evident the importance of the poling atmosphere.

For a more complete understanding we have studied the evolution of the nonlinear layer ( $\chi^{(2)}$  and thickness). The nonlinear layer was optically assessed using the Maker's fringes technique [11] and where necessary (the Maker's fringes technique does not provide enough resolution for thicknesses below 10  $\mu\text{m}$ , unless prism assisted [12]) the thickness was estimated by measuring

the SH intensity as a function of the etched layer. Fig.2 shows an example of Maker's fringes (SH signal as a function of incident angle) obtained for samples poled in air and in vacuum for 10 minutes. The position of the peaks is indicative for the thickness of the nonlinearity: it is clear from fig. 2 that the nonlinear layer for the sample poled in vacuum is wider than that for the sample poled in air. Assuming a uniform distribution of the nonlinear layer, from numerical simulation of the Maker's fringes, we estimated the thicknesses for the poled samples and, by comparing the SH signals with those generated by quartz, we calculate the values of  $\chi_{33}^{(2)}$ . Fig. 3 shows the  $\chi_{33}^{(2)}$  values as functions of the corresponding nonlinear thicknesses for different poling times, both for samples poled in air and vacuum. From fig.3 it is evident that the nonlinear thickness in air is always smaller than in vacuum for the same poling time and more importantly its growth in air is much slower than in vacuum. Correspondingly the  $\chi^{(2)}$  values in air are higher than in vacuum, as expected considering that most of the applied voltage drops across the depletion layer and that  $\chi^{(2)}$  is proportional to the electric field ( $E_{DC}$ ) stored in the depletion layer.

Laser induced pressure pulse (LIPP) measurements, based on the detection of current generated by charge displacement due to the propagation of a pressure pulse caused by a high power laser pulse hitting an absorbing target on the sample surface [9], were also carried out on the poled samples to determine the space-charge distribution induced by poling. Fig. 4 shows the results for the LIPP measurements for samples poled in air for 40 minutes (fig. 4a) and in vacuum for 10 minutes (fig.4b). The metal electrode is evaporated on the cathodic surface, so that the pressure pulse first propagates from the cathode to the anode, it bounces back from the anodic surface and travels toward the cathode, and this occurs periodically. The sign of the LIPP current signal is

the same as the sign of the charge. Therefore for the sample poled in air (fig. 4a) the charge distribution is made of positive charge near the anodic surface and negative charge located under the anodic surface. Taking account of the longitudinal sound velocity in fused silica ( $5.95 \cdot 10^3$  m/s) a thickness of about  $10 \div 15$   $\mu\text{m}$  has been calculated for the depletion region (distance between the positive and negative layer). In addition it is visible a smaller positive peak in the middle of the two positive anodic peaks (at  $\sim 30$  ns), indicating the presence of positive charge at the cathode. For the sample poled in vacuum (fig. 4b) the structure for the space-charge distribution under the anodic surface consists of a positive charge layer close to the anodic surface and two negative layers at a distance, from the positive layer, of  $10 \div 15$   $\mu\text{m}$  and  $30 \div 35$   $\mu\text{m}$  respectively. As expected there is remarkable agreement between the dimensions for the space charge field region (from LIPP measurements) and the nonlinear thickness estimated from Maker's fringes experiments, for both samples poled in air and vacuum. Moreover the LIPP signal, hence the density of charge, for samples poled in vacuum is smaller than that for samples poled in air. This is consistent with smaller  $\chi^{(2)}$  values.

The experimental results contained in this paper clearly point out that a single carrier model is inadequate to explain the mechanism of thermal poling. Such a model would imply the formation, within tens of seconds, of a negatively charged  $\text{Na}^+$  ions depleted region (few  $\mu\text{m}$  thick) under the anode where the nonlinearity would be confined. It would not explain the influence of the atmosphere on poling, the presence of slower processes than  $\text{Na}^+$  drift, the size of the nonlinear layer, and the multiple charge distribution detected in samples poled in vacuum. There are strong indications that other charged carriers are involved in the poling process [13] which is likely to take place in two stages: the rapid formation, within tens of seconds, of

negatively charged region depleted with cations ( $\text{Na}^+$ ) which cumulate and are neutralised at the cathode (see positive spike at  $\sim 30$  ns in fig.4a) followed by a slower process which is responsible for charge separation within the depletion region [5,6]. The time scale of the second stage depends on the charged species involved, on the poling atmosphere (air or vacuum) and on the poling conditions.

It has been proposed [6] that, during the second stage of thermal poling in air,  $\text{H}^+$  or  $\text{H}_3\text{O}^+$  are driven by the high electric field at the anode into the region depleted by  $\text{Na}^+$ , thus neutralizing the negative charges left behind by  $\text{Na}^+$ . At the same time, the region depleted with  $\text{Na}^+$  increases and this ion exchange process results in the forward movement of the negative depleted region. For increasing time, the nonlinear thickness increases, thus leading to a decrease of the electric field, hence of  $\chi^{(2)}$ . The poling stops when the electric field near the anode drops to values corresponding to which  $\text{H}^+/\text{H}_3\text{O}^+$  ions cannot be driven into the sample and when the total voltage drops across the depletion region, so that the movement of  $\text{Na}^+$  in the bulk stops. This multiple carriers model which considers  $\text{Na}^+$  and  $\text{H}^+/\text{H}_3\text{O}^+$  can explain our experimental results obtained for samples poled in air. However it does not explain why the poling in vacuum is faster (i.e. faster growth for the space-charge field region) and leads to a more complex charge distribution than in air. In addition in vacuum it is unlikely that  $\text{H}^+/\text{H}_3\text{O}^+$  species are significantly injected because of the low water concentration in the surrounding atmosphere and on the sample surface.

We believe that negative charged carriers, such as electrons [5,7] and oxygen ions [8], are likely to move in the depletion region because of the high field. The movement of these negative

carriers keep the electric field to levels below the breakdown field. Right after the Na<sup>+</sup> depleted region is formed, the electric field peaks at the anode surface causing currents of electrons or oxygen ions. Because of this, the peak of the electric-field moves further from the anode surface with increasing time, leading to an increase in the nonlinear thickness. Correspondingly the electric field and the  $\chi^{(2)}$  become smaller, while the resistivity in the depletion layer increases. The poling stops when the increase in resistivity and voltage in the depletion region makes negligible the Na<sup>+</sup> drift in the bulk of the sample. The described electric-field driven motion of negative charges is responsible for thermal poling in vacuum since the injection of H<sup>+</sup>/H<sub>3</sub>O<sup>+</sup> is limited, whereas in air atmosphere the latter is more significant. Because of the movement of negative charges in the depletion region the initial negative depletion layer can be split into two negative charged regions, i.e. the charge distribution of fig. 4b.

In conclusion, we have observed clear differences in the space charge distribution and in the value and location of the nonlinearity between fused silica samples thermally poled in air and in vacuum. The experimental results cannot be explained by a single Na<sup>+</sup>-carrier model, suggesting that other slower ionic species are involved in the process (H<sup>+</sup> or H<sub>3</sub>O<sup>+</sup> in air, whereas electrons or oxygen ions in vacuum). The time evolution of the nonlinear layer ( $\chi^{(2)}$  and thickness) has been studied in thin silica samples, i.e. similar geometry to fibres. This is relevant for improving the poling of fibre devices. In fact we have recently demonstrated record SH conversion efficiencies exceeding 20% in periodically poled germanosilicate fibres [14].

V. P. and F. S. acknowledge Pirelli Cavi for their fellowship and studentship respectively.

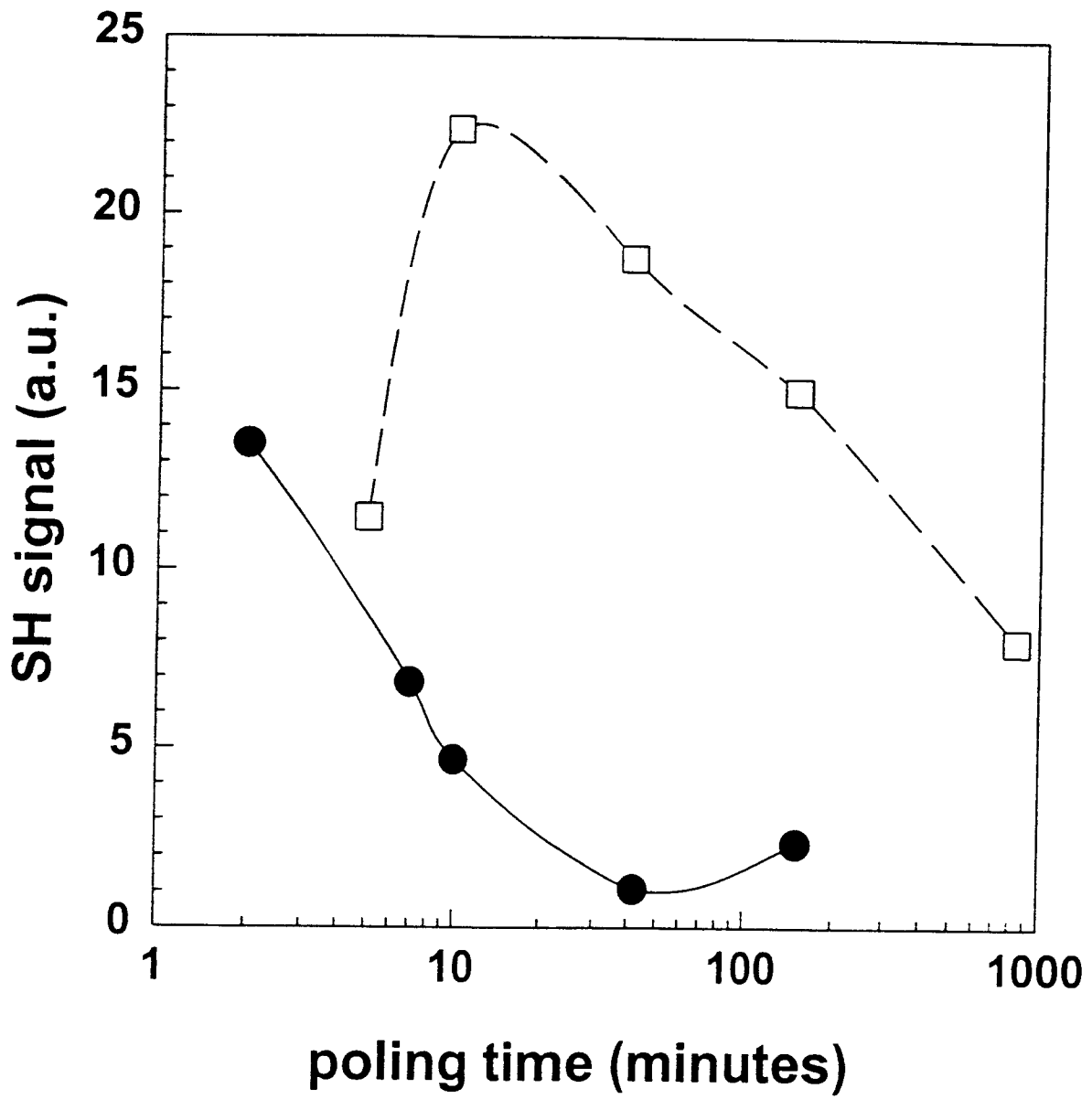
## References

1. R. A. Myers, N. Mukherjee, S.R.J. Brueck, *Optics Lett.* **16**, 1732 (1991).
2. A. Okada, K. Ishii, K. Mito, K. Sasaki, *Appl. Phys. Lett.* **60**, 2853 (1992).
3. P.G. Kazansky, A. Kamal, P. St. J. Russell, *Optics Lett.* **18**, 693 (1993).
4. T. Fujiwara, M. Takahashi, and A.J. Ikushima, *Electronics Lett.* **33**, 980 (1997).
5. H. Takebe, P.G. Kazansky, and P. St. J. Russell, *Optics Lett.* **21**, 468 (1995).
6. T.G. Alley, R.A. Myers, and S.R.J. Brueck, *OSA 1997 Technical Digest Series 17*, 293 (1997).
7. U.K. Krieger and W.A. Lanford, *J. Non-Cryst. Solids* **102**, 50 (1988).
8. D.E. Carlson, *J. Am. Ceram. Soc.* **57**, 291 (1974).
9. G.M. Sessler, J.E. West, G. Gerard, *Phys. Rev. Lett.* **48**, 563 (1982).
10. P.G. Kazansky, A.R. Smith, P.St.J. Russell, G.M. Yang, G.M. Sessler, *Appl. Phys. Lett.* **68**, 269 (1996).
11. P.D. Maker, R.W. Terhune, M. Nisenoff, C.M. Savage, *Phys. Rev. Lett.* **8**, 21 (1962).
12. D. Pureur, A.C. Liu, M.J.F. Digonnet, and G.S. Kino. *Optics Lett.* **23**, 588 (1998).
13. P.G. Kazansky, A. Kamal, P. St. J. Russell, *Optics Lett.* **18**, 1141 (1993). J.M. Dell, M.J. Joyce, and G.O. Stone, Australian Physical Society meeting, 1993.
14. V.Pruneri, G.Bonfrate, P.G.Kazansky, D.J.Richardson, N.G.Broderick, J.P.de Sandro, C.Simonneau, P.Vidakovic, and J.A.Levenson, to be published, *Optics Lett.*

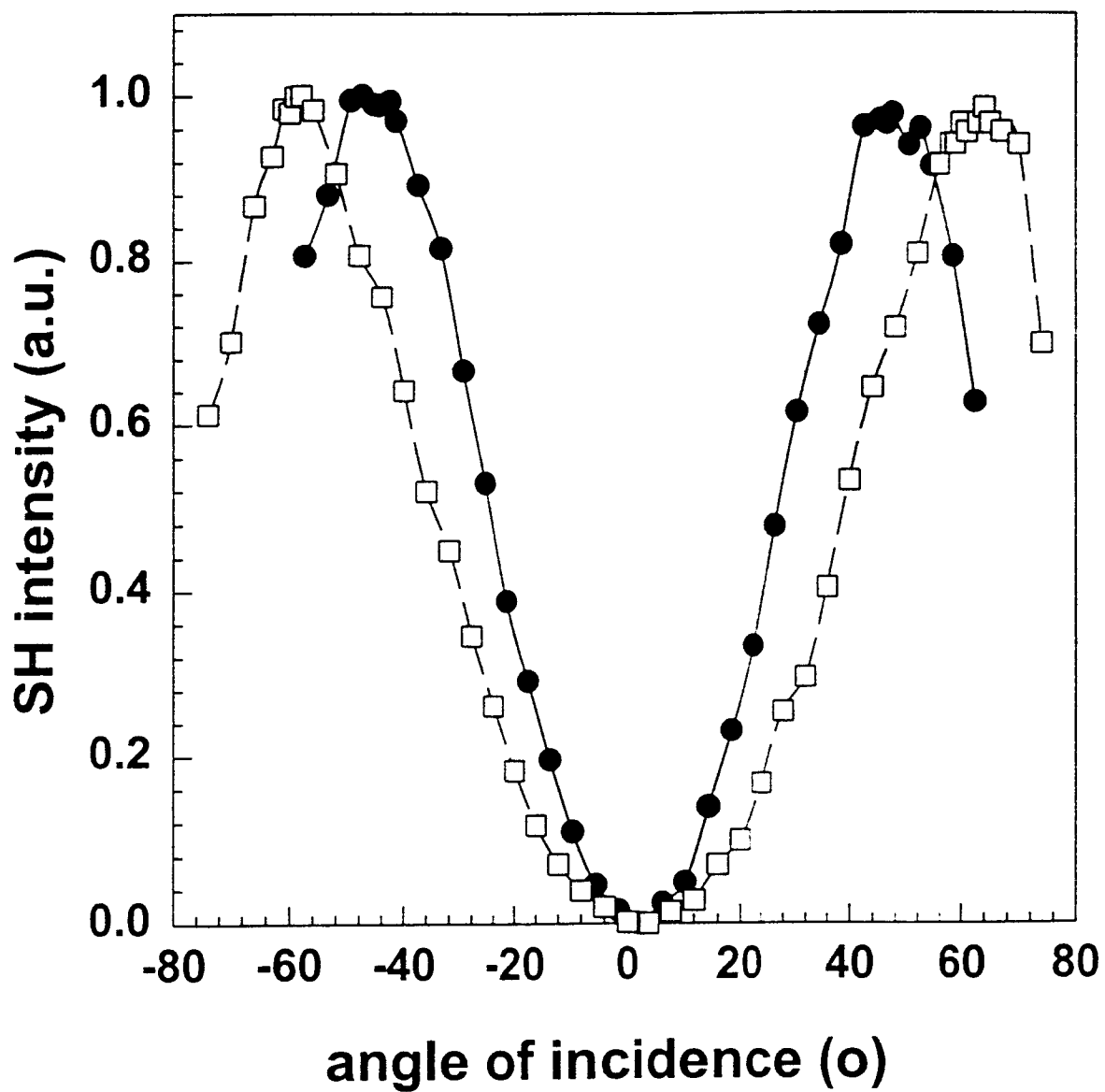


## Figure Captions

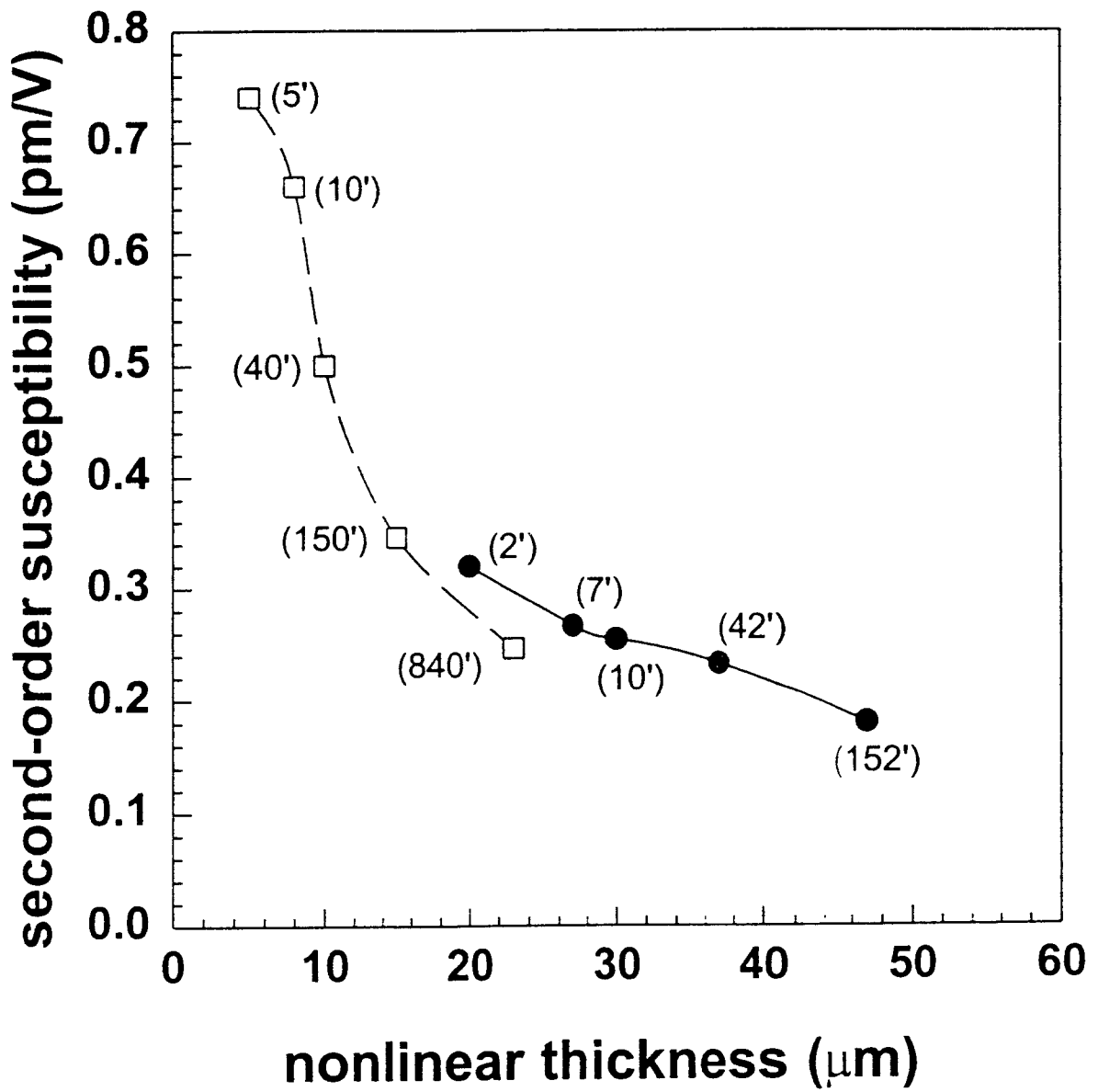
1. SH signal as a function of poling time for samples poled in air (open squares) and in vacuum (filled circles). All samples were poled with 4 kV at 290 °C and vacuum pressure is  $\sim 10^{-8}$  atm. The values of SH signal are the maximum values obtained by optimizing the angle of incidence.
2. Maker's fringes for sample poled in air (open squares) and in vacuum (filled circles) for the same poling time (10 min), voltage (4 kV) and temperature (290 °C).
3. Second-order nonlinear optical susceptibility ( $\chi_{33}^{(2)}$ ) as a function of nonlinear thickness for different poling times (in brackets), for samples poled in air (open squares) and in vacuum (filled circles). The nonlinear coefficient  $d_{33}$  is  $\sim \chi_{33}^{(2)}/2$
4. LIPP measurement when the pressure pulse is launched from the cathode side for a sample poled in air at 4 kV, 290 °C, 40 minutes (a) and in vacuum at 4 kV, 290 °C, 10 minutes, and  $10^{-8}$  atm (b). The positive and negative peaks are caused by positive and negative charge layers respectively. The insets represent the corresponding charge distributions in the samples. The positive overshoots in (b) are artifacts, which do not indicate positive charge.



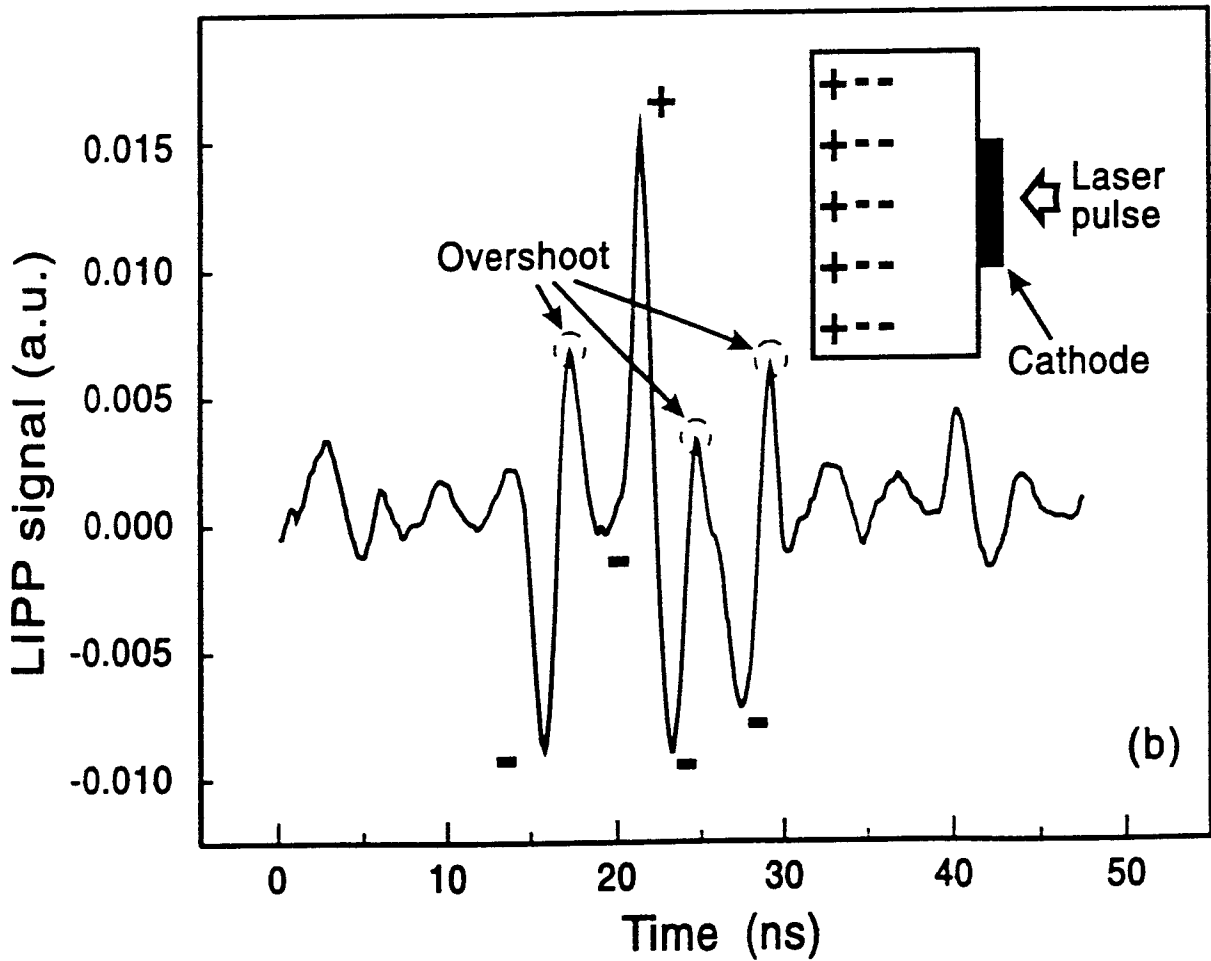
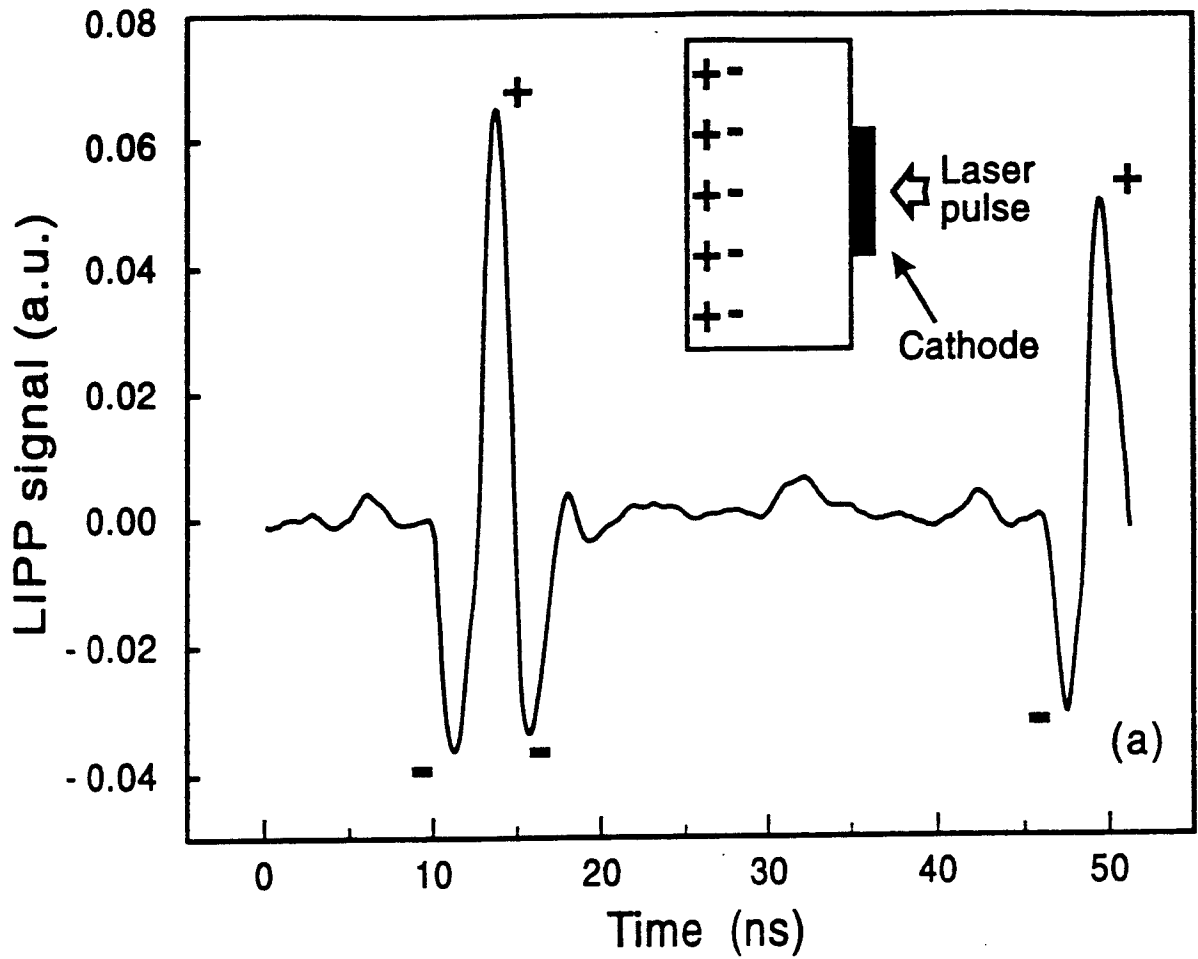
Pruneri et al., fig.1



Pruneri et al., fig.2



Pruneri et al., fig.3



Pruneri et al., fig.4